A Sustainable Production of H_2 by Water Splitting and Photo-Reforming of Organic Wastes on Au/TiO$_2$ Nanotube Arrays

Claudio Ampelli*, Chiara Genovese, Paola Lanzafame, Siglinda Perathoner, Gabriele Centi

Department of Electronic Engineering, Chemistry and Industrial Engineering, University of Messina
Viale F. Stagno D'Alcontres 31 - 98166 Messina, Italy
ampellic@unime.it

We report here on the sustainable production of hydrogen by the use of nano-ordered TiO_2 arrays doped with gold nanoparticles (Au NPs). The presence of a nano-architecture in TiO_2 substrate may strongly improve the ability to disperse the Au NPs on its surface, which act as electron-attractive centres for the reduction of protons. We prepared the TiO_2 nanotube arrays by controlled anodic oxidation starting from Ti foils and deposited the Au NPs by pre-preparing gold colloidal solutions. The samples were characterized by Transmission Electron Microscopy (TEM), UV-Visible Diffusive Reflectance Spectroscopy, Cyclic Voltammetry and Chronoamperometry. Then, they were tested within our homemade photo-electrochemical (PEC) reactors in water photo-splitting, as well as in photo-dehydrogenation of ethanol for H_2 production. A solar simulator was used to evaluate their photo-responses in different absorption regions (ultraviolet or visible part). Results evidenced that smaller Au NPs strongly enhanced titania performances under visible light irradiation, opening the route of a feasible implementation of the PEC devices in the energy recovery from organic waste solutions (i.e. from biomass processing) that are too dilute to be processed by conventional routes.

1. Introduction

Solar energy is undoubtedly the more promising alternative option to fossil fuels for the future global economy. The amount of sunlight striking continuously the Earth's surface can be considered as an abundant, largely untapped energy resource (Genovese et al., 2013a) and research progress has evidenced that direct conversion of solar to chemical energy may be performed in an one-step process by water photo-electrolysis (process intensification). Unfortunately, the photo-active materials currently used to harvest sunlight and split water, are poorly efficient under visible illumination (Ampelli et al., 2011a). The more known example is titania (TiO_2), a promising semi-conductor material but limited by its high band gap (~3.2 eV) which sets its light absorption within the ultraviolet region of the electromagnetic spectrum. Several attempts have been in literature to extend the cut-off wavelength of this catalyst, including doping the crystalline lattice with hetero-atoms or decorating its surface with metal nanoparticles (NPs), but only slight improvements have been resulted (Passalacqua et al., 2012). Among the other metals, Au represents a special case; though it is well known that Au NPs positively influence solar light harvesting of titania through surface plasmon resonance, the mechanism of interaction of the plasmons with the conduction band of titania has not unequivocally interpreted yet (Tian and Tatsuma, 2005). Contrasting explanations have been given to interpret visible light enhancement of Au NPs, but it is agreed that their size and dispersion, together with the titania morphology, are fundamental for obtaining good responses in terms of light absorption and photo-catalytic response. Recently, Notarianni et al. (2013) showed that concentration, size and geometry of Au NPs are key factors that directly influence the light absorption in organic solar cells. The correct choice of size, concentration and location of Au NPs resulted in an enhancement of the power conversion efficiencies. Min et al. (2009) observed that Au NPs supported on

titania promoted the 1,4-dioxane photocatalytic degradation. This beneficial effect of gold was found to originate from its surface plasmon resonance, and its magnitude depended on both density and size of Au NPs. Those examples showed that is possible tuning the characteristics and properties of Au TiO_2 by adopting the proper synthetic methodology and adjusting the parameters during its preparation.

In this contribution we have investigated the photo-response enhancement of Au-doped titania nanodimensional materials, to be processed in the production of H_2 by water splitting. In order to obtain Au NPs with different dimensions, we started to synthesize colloidal solutions of Au NPs by reduction of an aqueous solution of $HAuCl_4$ with $NaBH_4$ or sodium citrate. By varying some parameters, such as the i) nature of reducing/capping agent, ii) ratio of gold ion concentration to stabilizer/reductant and iii) reaction temperature, a high grade of control on dimension and size distribution may be obtained. In a second step an appropriate volume of Au colloidal solution was contacted with the TiO_2 substrate.

Gold-TiO_2 samples were tested in the process of water photo-electrolysis, but H_2 productivity can strongly be increased if organic compounds (also in low concentrations) are added in the reaction mixture (Ampelli et al., 2013a). The photo-reforming of organics may represent a good opportunity to recover waste streams coming from biomass processing (agro-food or agro-chemical) which are too dilute to be processed by conventional catalytic routes, i.e. as feed to produce H_2 by catalytic processes or methane by anaerobic digestion, or to be used as feed in the new generation of fuel cells (Ampelli et al., 2011b). From a practical perspective, it would also be interesting the possibility of co-producing, together with H_2, valuable chemicals rather than carbon dioxide, in order to have better process economics. A good example could be the photocatalytic dehydrogenation of ethanol to H_2 and acetaldehyde, as alternative to the ethanol photoreforming (Ampelli et al., 2014). In terms of product value at current costs (assuming 100 % selectivity in both the reactions), photo-dehydrogenation has an economic value about 3.0-3.5 times higher than photoreforming (Ampelli et al., 2013b).

The combination of Au NPs and nanostructured TiO_2 ordered arrays may have a positive effect in the enhancement of the activity of these photo-catalysts, which are very promising for a real implementation of photo-electrochemical (PEC) systems for a sustainable production of energy (Genovese et al., 2013b).

2. Experimental

2.1 Synthesis of Au-TiO_2

We started preparing the colloidal solutions containing size-controlled Au NPs. In order to obtain metal particles with different dimensions (ranging from 2 to 40 nm), the colloidal solutions were prepared according to three different procedures. In the first procedure, a freshly prepared aqueous solution of $NaBH_4$ (2 mM, 30 mL) was cooled in an ice bath. Next, a solution of $HAuCl_4 \cdot 3H_2O$ (1 mM, 10 mL) was added drop to drop to the reducing solution while stirring. The solution turned pink indicating the formation of NPs (Lee and Meisel, 1982). This solution is indicated hereinafter as Au@SB. In the second procedure, a solution of $HAuCl_4 \cdot 3H_2O$ (1 mM, 90 mL) was heated at 100 °C for 15 min in an oil bath, then a solution of sodium citrate (38.8 mM, 10 mL) was added. The mixture was maintained under reflux condition for 30 min. The oil bath was removed and stirring was continued for an additional 15 min (Grabar et al., 1995). This solution is indicated hereinafter as Au@SC. In the third procedure, Au NPs were stabilized by Polyvinylpyrrolidone (PVP). $HAuCl_4 \cdot 3H_2O$ (16 mM, 25 mL) was added to 106 mg of PVP aqueous solution (300 mL) with stirring for 30 min. An aqueous solution of $NaBH_4$ (100 mM, 5 mL) was rapidly added and the mixture was stirred for 3 h (Yogi et al., 2011). This solution is indicated hereinafter as Au@PVP.

In a second step of the preparation, an appropriate volume of the Au NPs colloidal solutions was contacted with TiO_2 powder (P25 Degussa), in order to have a Au loading of 0.5 wt. % by wet impregnation at 90 °C (Ampelli et al., 2012a). Moreover, it is well known that the presence of an ordered nano-architecture in the TiO_2 substrate may strongly increase the efficiency of light harvesting. Thus, we prepared TiO_2 nanotube ordered arrays by controlled anodic oxidation starting from Ti foils (Shankar et al., 2009) and studied the enhancement of the photo-response under visible irradiation by depositing the size-controlled Au NPs onto the TiO_2 nanotube surface (with a Au loading of 0.5 mg per cm^2 on titania). The preparation of TiO_2 nanotube arrays was reported elsewhere (Ampelli et al., 2009).

2.2 Characterization

The materials were characterized by nitrogen adsorption–desorption isotherms according to the conventional Brunauer-Emmet and Teller (BET) surface area analysis, using a Micromeritic ASAP 2010 after degassing the samples overnight at 350 °C. Ultraviolet-visible diffuse reflectance spectra were recorded by a Jasco V570 spectrometer equipped with an integrating sphere for solid samples using $BaSO_4$ as reference and in air. Transmission electron microscopy (TEM) images were acquired by using a Philips CM12 microscope (resolution 0.2 nm) with an accelerating voltage of 120 kV, while the elemental analysis was investigated by using a Philips XL-30-FEG scanning electron microscope (SEM) equipped

with an energy-dispersive X-ray (EDX) analyzer. Cyclic Voltammetry and Chronoamperometry measurements were performed by using a three-electrode photo-electrochemical cell, with a Pt wire as counter-electrode and a KCl saturated Ag/AgCl reference electrode. All the tests were performed at room temperature in 1 M KOH solution at a 15 mV s^{-1} scan rate in the potential range ±1.5 V using a 2049 AMEL potentiostat–galvanostat.

2.3 Apparatus for Testing

The experimental apparatus for the photo-catalytic experiments consists of a solar illuminator, a photo-reactor and a gas chromatograph for the analysis.

The solar illuminator is a Xe-arc lamp (ORIEL, 300 W) equipped with a set of lenses for light collection and focusing, and a water filter to eliminate the infrared radiation. According to the nature of the Au-TiO$_2$ sample, i) a powder or ii) a thin film, we used two different photo-reactors: a conventional slurry photo-reactor and a homemade PEC reactor, respectively.

The PEC reactor is made of Plexiglas and equipped with a quartz window. It has a two-electrode configuration with two compartments for separated evolution of H$_2$ and O$_2$. The irradiated area is 5.7 cm^2. The principle of working of the PEC device was previously reported (Ampelli et al., 2012b).

A gas chromatograph (GC) with a Thermal Conductivity Detector (TCD) was used to analyse the permanent gases (H$_2$, O$_2$, CH$_4$ and CO) by a molecular sieve column (5A Plot). Carbon dioxide, ethanol and acetaldehyde were instead analysed by a fused silica column (Rt-Qbond).

3. Results

3.1 BET and XRD Analysis

The BET analysis of commercial TiO$_2$ P25 Degussa showed a 48 m^2 g^{-1} specific surface area, while results for Au doped TiO$_2$ powders were slightly lower (38-43 m^2 g^{-1}), probably due to a partial aggregation of particles after the wet impregnation. The crystallinity of the Au/TiO$_2$ samples was studied by powder X-ray diffraction (XRD) measurements: according to those measurements, the Au/TiO$_2$ powders displayed the typical mixed phase composition of TiO$_2$ P25 Degussa, consisting in about 80 % *anatase* and 20 % *rutile*. This leads to the conclusion that the structure of titania did not undergo significant alterations during the synthetic process. The mean crystallite size is about 20-25 nm for all the samples.

3.2 UV-Visible Diffuse Reflectance Spectroscopy

Figure 1a shows the absorption spectra of the colloidal solutions prepared according to the three different procedures of synthesis. For all the spectra, an absorption band is clearly visible in the range 500-600 nm, due to the plasmon absorption of Au NPs. The maximum values of those peaks occurred at 511 nm for Au@SB, 520 nm for Au@SC and 530 nm for Au@PVP, the wavelength depending on the size of the Au NPs. Thus, a high grade of control on dimension and size distribution may be obtained by changing the nature of reducing and capping agent, the ratio of gold ion concentration to stabilizer/reductant and the reaction temperature, as evidenced by the plasmon red-shift from 511 to 530 nm.
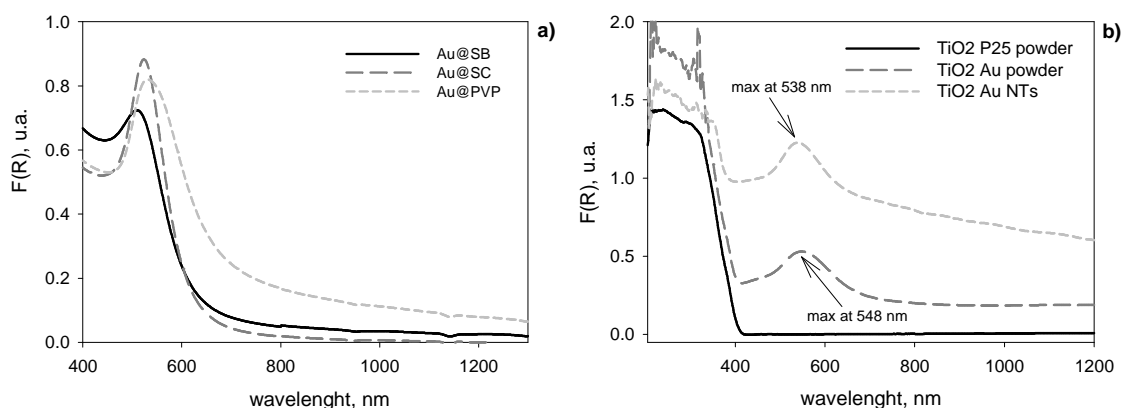

Figure 1: UV-visible absorption spectra for a) the three gold colloidal solutions Au@SB, Au@SC and Au@PVP, and for b) Au/TiO$_2$ photocatalysts (powder and nano-ordered thin film) obtained by impregnation from Au@SC colloidal solution
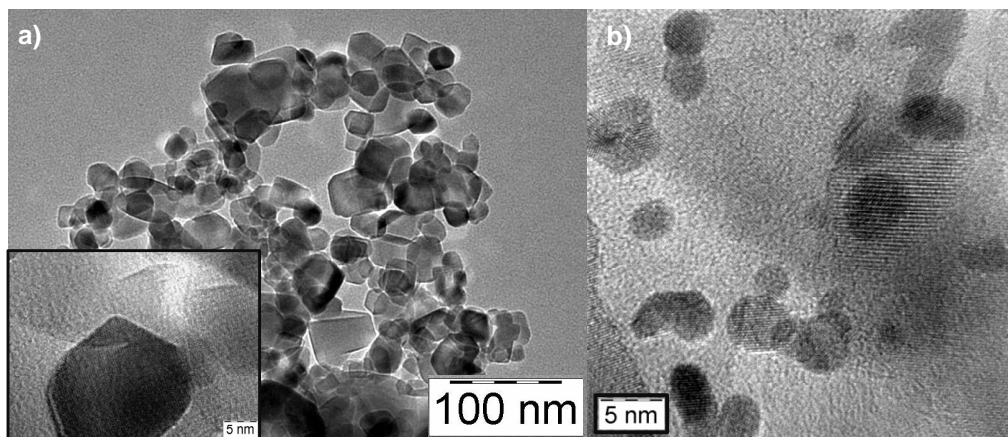
Figure 2: Representative TEM image of a) Au/TiO$_2$ powder (in the insert a TEM image with higher magnification) and b) nano-ordered Au/TiO$_2$ film, prepared from Au@SB colloidal solution

Then, the gold colloidal solutions having size-controlled Au NPs were deposited on TiO$_2$ substrate. Figure 1b shows the absorption spectra of Au/TiO$_2$ powder and nanotube arrays prepared by impregnation from Au@SC colloidal solution. For reference, the spectrum of TiO$_2$ P25 Degussa is also reported. The intense band below 400 nm is due to the absorption of the TiO$_2$ semiconductor. The band is centred at about 350 nm and is related to the lowest energy charge transfer Ti^{4+}→O^{2-}. For the bare TiO$_2$ (P25 Degussa) the band gap could be estimated to be in the 3.0-3.1 eV range, consistent with expectations for a mixture of *anatase* and *rutile* TiO$_2$ polymorphs. The presence of Au NPs shifted the band gap to about 2.9 eV, while the shift was higher for the nano-ordered Au/TiO$_2$ film (~2.8 eV).

Gold/TiO$_2$ samples also exhibited a broad absorption in the visible region (in the range 500-650 nm), which is attributable to the surface plasmon band of Au NPs. Comparing to the colloidal solution, the maximum value for Au/TiO$_2$ powder occurred at higher wavelengths, as Figure 1b shows for Au@SC (548 vs. 520 nm), probably for a partial aggregation of the Au NPs during the wet impregnation. This last phenomenon is strongly minimized for the Au/TiO$_2$ nanotube film (maximum at 538 nm), as the presence of a one-dimensional nano-architecture in TiO$_2$ allowed a better dispersion and localization of the Au NPs.

3.3 Transmission Electron Microscopy (TEM)

The analysis by TEM showed that rather small metal particles, well dispersed over crystalline TiO$_2$ phase, are present for all the Au/TiO$_2$ samples and no abnormally large particles or many aggregates were observed. As an example, Figure 2 reported TEM images of Au/TiO$_2$ samples prepared with Au@SB colloidal solution, consisted of a) titania powder with small deposited Au NPs (~18-22 nm) and b) smaller Au NPs on a single TiO$_2$ nanotube. The insert in Figure 2a reports a magnification of a TEM image showing a well-rounded Au particle of 20 nm diameter, while Au NPs on TiO$_2$ nanotubes have an average diameter of ~5 nm, confirming the UV-Visible results. The nanometer-sized Au NPs are known to exert visible-light absorption, a phenomenon which is due to the surface plasmon resonance.

3.4 Photo-current measurements

To be used as photo-catalysts in PEC devices, the Au/TiO$_2$ samples should have a good absorption of solar light, but also a sharp charge separation (electrons and holes) is needed for the reactions of oxidation/reduction. Due to the vectorial transport of electrons in nanotubes with respect to a random assembly of particles, nano-ordered Au/TiO$_2$ films are more suitable for PEC application, as their nano-structure minimizes the charge recombination at the grain boundaries (Natali Sora et al., 2013).

Figure 3a shows the photo-current profiles obtained by cyclic voltammetry analysis for the nano-ordered Au/TiO$_2$ film obtained by impregnation of Au@SC (the dark profiles are also reported). During the positive scan, the Au/TiO$_2$ film showed a main anodic peak centred at 0.06 V, probably due to the formation of a monolayer of adsorbed hydroxyl species OH$^-$ on the Au NPs. The oxidation of OH$^-$ was favoured by the electronic hole formation for charge separation in TiO$_2$ when irradiated by UV-visible light.

Figure 3b shows the chronoamperometric measurements for the same sample. The ON/OFF illumination displayed an instantaneous rise in photocurrent and quick recovery to the original photocurrent value through multiple ON/OFF cycles. The monitoring during discontinuous illumination revealed stability and reproducibility of the photocurrent in all the tested samples.
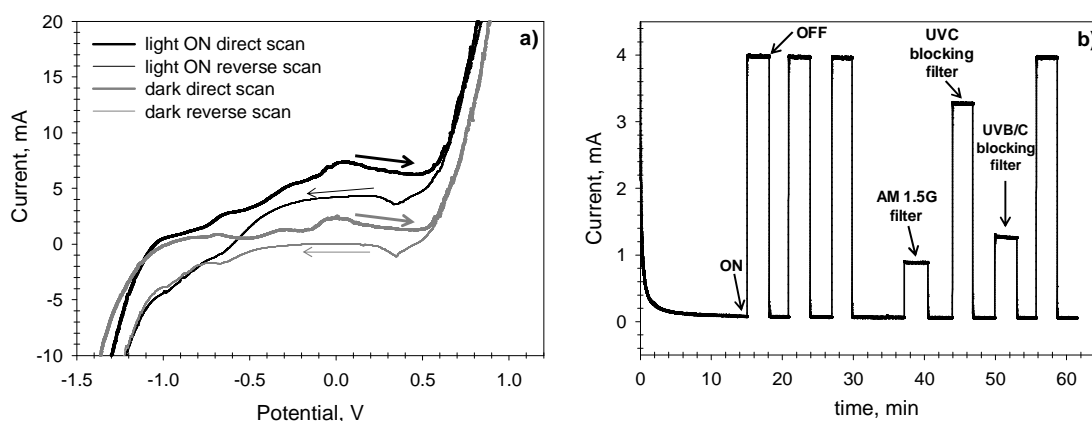
Figure 3: a) Cyclic voltammetric and b) chronoamperometric profiles for the nano-ordered Au/TiO₂ sample prepared by Au@SC, in dark and light (potential range ±1.5 V, scan rate 15 mV/s, 1 M KOH)

However, the most important result was the high percentage (22.3 % with respect to an open filter) of photocurrent obtained when an AM 1.5G filter (simulating standard terrestrial solar irradiance distribution) was used, due to the presence of very small Au NPs on the TiO₂ surface.

3.5 H₂ photo-production by water splitting and ethanol dehydrogenation

Photoelectrochemical (PEC) devices are emerging as promising and sustainable systems for solar H₂ generation. A well-designed photo-catalyst and a suitable photo-reactor (developed on purpose to maximize the photocatalytic performances), are together the key to enhance the H₂ productivity. For that reason, we investigated the behaviour of Au/TiO₂ powders and films using two different photo-reactor configurations, as described in the experimental part. Table 1 reported the values of H₂ productivity obtained irradiating the various photo-catalysts in water photo-electrolysis and ethanol dehydrogenation (10 vol. % ethanol) processes.

Table 1: Hydrogen productivity for Au/TiO₂ powders and films in different photo-reactors and processes

process	sample nature	colloidal synthetic solution	H_2 $\mu mol\ h^{-1}$	CH_3CHO $\mu mol\ h^{-1}$
water photo-electrolysis	powder in suspension	Au@SB	9.6	-
		Au@SC	7.2	-
		Au@PVP	6.5	-
	thin film of nanotube arrays	Au@SB	15.0	-
		Au@SC	10.8	-
		Au@PVP	10.2	-
ethanol photo-dehydrogenation	powder pressed on a glass layer	Au@SB	147.0	108.0
		Au@SC	109.2	69.3
		Au@PVP	105.3	67.8

Even if the photo-reactors used for testing the samples are different, the irradiated area, the incident light and the amount of photocatalyst were maintained as constant; thus, data of H₂ productivity are comparable. Results showed that Au/TiO₂ nanotube arrays prepared by Au@SB colloidal impregnation are the best photocatalysts investigated for the water photo-electrolysis process, because of the high surface plasmon resonance effect due to the presence of very small Au NPs. In presence of ethanol, H₂ productivity increased of about one order of magnitude, with the simultaneous production of a valuable product such as acetaldehyde.

4. Conclusions

In this contribution we have studied the enhancement of titania photo-response under simulated solar irradiation, by depositing size-controlled Au NPs on TiO₂ Degussa P25 and on ordered arrays of TiO₂ nanotubes. The Au NP size and dispersion on titania surface (obtained by changing some synthetic

parameters starting from three different gold colloidal solution), together with a highly ordered nanoarchitecture of TiO_2-based substrate (obtained by controlled anodic oxidation of Ti foils), are of paramount importance to enhance the activity of these photo-catalysts. In the view of a biomass utilization, the presence of organics may strongly enhance the H_2 productivity; thus, photo-degradation of waste streams coming from biomass processing may be a sustainable solution to produce H_2 and acetaldehyde (in the case of bioethanol).

References

Ampelli C., Passalacqua R., Perathoner S., Centi G., 2009, Nano-engineered materials for H_2 production by water photo-electrolysis, Chemical Engineering Transactions, 17, 1011-1016.

Ampelli C., Passalacqua R., Genovese C., Perathoner S., Centi G., 2011a, A novel photo-electrochemical approach for the chemical recycling of carbon dioxide to fuels, Chemical Engineering Transactions, 25, 683-688.

Ampelli C., Passalacqua R., Perathoner S., Centi G., 2011b, Development of a TiO_2 nanotube array-based photo-reactor for H_2 production by water splitting, Chemical Engineering Transactions, 24, 187-192.

Ampelli C., Spadaro D., Neri G., Donato N., Latino M., Passalacqua R., Perathoner S., Centi G., 2012a, Development of Hydrogen Leak Sensors for Fuel Cell Transportation, Chemical Engineering Transactions, 26, 333-338.

Ampelli C., Genovese C., Passalacqua R., Perathoner S., Centi G., 2012b, The use of a solar photoelectrochemical reactor for sustainable production of energy, Theor. Found. Chem. Eng., 46 (6), 651-657.

Ampelli C., Passalacqua R., Genovese C., Perathoner S., Centi G., Montini T., Gombac V., Fornasiero P., 2013a, Solar energy and biowaste conversion into H_2 on CuO_x/TiO_2 nanocomposites, Chemical Engineering Transactions, 35, 583-588.

Ampelli C., Passalacqua R., Genovese C., Perathoner S., Centi G., Montini T., Gombac V., Delgado J.J., Fornasiero P., 2013b, H_2 production by selective photo-dehydrogenation of ethanol in gas and liquid phase on CuO_x/TiO_2 nanocomposites, RSC Advances, 3 (44), 21776-21788.

Ampelli C., Genovese C., Passalacqua R., Perathoner S., Centi G., 2014, A gas-phase reactor powered by solar energy and ethanol for H_2 production, Appl. Therm. Eng., DOI: 10.1016/j.applthermaleng.2014.04.01, in press.

Genovese C., Ampelli C., Perathoner S., Centi G., 2013a, Electrocatalytic conversion of CO_2 on carbon nanotube-based electrodes for producing solar fuels, J. Catal., 308, 237-249.

Genovese C., Ampelli C., Perathoner S., Centi G.. Electrocatalytic conversion of CO_2 to liquid fuels by using nanocarbon-based electrodes, 2013b, J. Energy Chem., 22 (2), 202-213.

Grabar K.C., Freeman G.R., Hommer M.B., Natan M.J., 1995, Preparation and Characterization of Au Colloid Monolayers, Anal. Chem., 67, 735-743.

Lee P.C., Meisel D., 1982, Adsorption and Surface-Enhanced Raman of Dyes on Silver and Gold Sols, J. Phys. Chem., 86, 3391-3395.

Min B.K., Heo J.E., Youn N.K., Joo O.S., Lee H., Kim J.H., Kim H.S., 2009, Tuning of the photocatalytic 1,4-dioxane degradation with surface plasmon resonance of gold nanoparticles on titania, Catalysis Communications, 10, 712-715.

Natali Sora I., Fontana F., Passalacqua R., Ampelli C., Perathoner S., Centi G., Parrino F., Palmisano L., 2013, Photoelectrochemical properties of doped lanthanum orthoferrites, Electrochim. Acta, 109, 710-715.

Notarianni, M., Vernon K., Chou A., Aljada M., Liu J., Motta N., 2013, Plasmonic effect of gold nanoparticles in organic solar cells, Sol. Energy, DOI: 10.1016/j.solener.2013.09.026.

Passalacqua R., Ampelli C., Perathoner S., Centi G., 2012, Anodically Formed TiO_2 Thin Films: evidence for a multiparameter dependent photocurrent-structure relantionship, Nanosci. Nanotechnol. Lett., 4,142-148.

Shankar K., Basham J.I., Allam N.K., Varghese O.K., Mor G.K., Feng X., Paulose M., Seabold J.A., Choi K.-S., Grimes C.A., 2009, Recent Advances in the Use of TiO_2 Nanotube and Nanowire Arrays for Oxidative Photoelectrochemistry, J. Phys. Chem. C, 113, 6327-6359.

Tian Y., Tatsuma T., 2005, Mechanisms and applications of plasmon-induced charge separation at TiO_2 films loaded with gold nanoparticles, J. Am. Chem. Soc., 127, 7632-7637.

Yogi C., Kojima K., Hashishin T., Wada N., Inada Y., Della Gaspera E., Bersani M., Martucci A., Liu L., Sham T., Over H., 2011, Size Effect of Au Nanoparticles on TiO_2 Crystalline Phase of Nanocomposite Thin Films and Their Photocatalytic Properties, J. Phys. Chem. C, 115, 6554-6560.